

# AMERICAN JOURNAL OF Botany

---

Computer Simulation of Branch Interaction and Regulation by Unequal Flow Rates in Botanical Trees

Author(s): Hisao Honda, P. B. Tomlinson and Jack B. Fisher

Source: *American Journal of Botany*, Vol. 68, No. 4 (Apr., 1981), pp. 569-585

Published by: Botanical Society of America, Inc.

Stable URL: <http://www.jstor.org/stable/2443033>

Accessed: 24-10-2016 15:14 UTC

## REFERENCES

Linked references are available on JSTOR for this article:

[http://www.jstor.org/stable/2443033?seq=1&cid=pdf-reference#references\\_tab\\_contents](http://www.jstor.org/stable/2443033?seq=1&cid=pdf-reference#references_tab_contents)

You may need to log in to JSTOR to access the linked references.

---

JSTOR is a not-for-profit service that helps scholars, researchers, and students discover, use, and build upon a wide range of content in a trusted digital archive. We use information technology and tools to increase productivity and facilitate new forms of scholarship. For more information about JSTOR, please contact [support@jstor.org](mailto:support@jstor.org).

Your use of the JSTOR archive indicates your acceptance of the Terms & Conditions of Use, available at

<http://about.jstor.org/terms>



*Botanical Society of America, Inc.* is collaborating with JSTOR to digitize, preserve and extend access to *American Journal of Botany*

## COMPUTER SIMULATION OF BRANCH INTERACTION AND REGULATION BY UNEQUAL FLOW RATES IN BOTANICAL TREES<sup>1</sup>

HISAO HONDA<sup>2</sup>, P. B. TOMLINSON, AND JACK B. FISHER

Harvard Forest, Harvard University, Petersham, Massachusetts 01366;  
and Fairchild Tropical Garden, Miami, Florida 33156

### ABSTRACT

Two aspects of branch interaction in trees are investigated theoretically. In the first it is assumed that there is a controlling factor in which the proximity of neighboring terminal branch units influences their branching capability. The almost horizontal tiers of lateral branches of *Terminalia catappa* L. and *Cornus alternifolia* L. are simulated by computer using values based on the measured branch geometries of real trees. For branch interaction, we assume a horizontal circle of inhibition whose center is the existing terminal point of a branch. If the end point of another branch extends into the circle, the original branch fails to bifurcate. Examples of computer simulated patterns are illustrated using different degrees of interference and are compared with branch tiers in *T. catappa*. In the second model the ability of a terminal branch unit to bifurcate is considered to be determined by the accumulation of a critical amount of a hypothetical growth- or bifurcation-determining factor. The daughter branches of a bifurcation are assumed to have differing "flow rates," i.e., the factor is distributed in different amounts between different daughter axes. Some simulated patterns generated by this model are very similar to real patterns found in *T. catappa* and an unnamed species of *Tabernaemontana*. In both simulations bifurcation ratios are determined and are shown to be a variable, not a fixed, property of the simulated trees.

A TREE can be regarded conceptually as a system of axes which develops by a process of repeated branching or bifurcation. In botanical trees the frequency of branching is almost never the same at every terminal branch. Thus, the number of terminal branches does not increase by a regular exponent ( $2^N$ ) since the rate of increment normally decreases. In the simplest analysis, this decrease can be attributed to two theoretical constraints on growth: 1) an environmental or exogenous factor, resulting in inter-branch (inter-meristem) competition or interaction such that the actual number of permanent branches falls with increasing age as a result of abortion and abscission of both young and old branches, and 2) an intrinsic or endogenous factor, by which two daughter

branches from one mother branch differentiate into different kinds of branches, one of which bifurcates less frequently than the other. This fundamental difference in frequency of branching is explained by us theoretically as a result of different flow rates through branch pairs.

In this paper we will investigate both constraints by using a tree model for computer simulation. The parameter values used in the model are obtained from three species of real trees, *Cornus alternifolia*, *Tabernaemontana* sp. and *Terminalia catappa*. Results of computer simulations are analyzed in terms of the number of terminal branches and the value of bifurcation ratios to allow some comparison with real trees. These ratios are indices which have been widely applied to tree systems, but we will show they have limited usefulness for understanding botanical trees.

Computer simulation has shown that quite simple algorithms may be used to generate three-dimensional branching patterns which closely resemble actual trees (Honda, 1971). The method, therefore, offers techniques for investigating developmental rules that govern the form of botanical trees and, by varying chosen parameters one at a time, gives insight into the adaptive nature of tree form. The influence which variations in normal developmental processes can have on tree form can thus be investigated in a preliminary but very

<sup>1</sup> Received for publication 18 April 1980; revision accepted 2 August 1980.

The main part of the present work was carried out during the stay of H. Honda at Harvard Forest as a research fellow of the Charles Bullard Fund of Harvard University. Additional support was provided by the Atkins Garden Fund and Cabot Foundation of Harvard University. The contribution of J. B. Fisher was supported in part by NSF grants DEB77-13953 and 79-14635. Acknowledgement is due to Mmes. D. R. Smith (Harvard Forest), M. Hayashi-Okuda, and T. Kondo, Misses K. Fukuda, M. Noda, K. Tanaka, Y. Tanaka, and Y. Ueura (Kanebo Institute for Cancer Research) for assistance.

<sup>2</sup> Permanent address: Kanebo Institute for Cancer Research, Misakicho 1-9-1, Kobe 652, Japan.

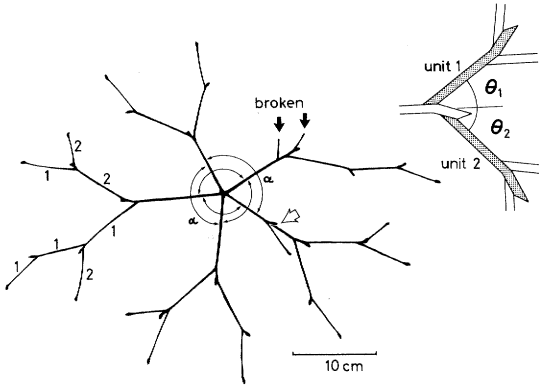


Fig. 1. *Cornus alternifolia*, branch tier of young tree viewed from above. Successively produced lateral branch complexes form a divergence angle,  $\alpha$  (shown by arcs), with each other. Branch units 1 and 2 indicated in one lateral branch complex (left). Solid arrows: broken branches. Open arrow: superposed lateral branch complexes. Drawn from a photograph taken at Harvard Forest in April, 1979. Insert: schematic explanation of the branch units 1 and 2 and their branching angles,  $\theta_1$  and  $\theta_2$ .



Fig. 2. *Cornus alternifolia*, branch tier from side; a photograph taken at Harvard Forest in June, 1979.

daughter axis is  $N + 1$ ; Rule 3 says that the sign of the branch angles changes at every branch order, so that a zigzag main axis of unit 1's with alternating direction is formed. In the basic model, every terminal branch unit bifurcates without limitations. In this first modified

economical way. The method becomes valuable when it is used to compare measured values from real trees.

**METHODS**—The symbols and parameters used in the analyses are summarized in Table 1.

Calculations were carried out by IBM system 370 at the Harvard University Office of Information Technology. Simulations were drawn by an electronic digital microcomputer with a disc memory (P652 and DAS 604, Olivetti) and an XY plotter (WX 535, Watanabe Sokuki, Tokyo).

**BRANCH INTERACTIONS**—*Branch geometry of Terminalia*—Computer simulations of the three-dimensional branching pattern of *Terminalia catappa* L. have been described by Fisher and Honda (1977). The same basic model and the branching rules 1 and 3 have been used in the present study for a horizontal branch tier of alternate symmetry, as described in detail by Fisher and Honda (1979). A young tree consists of an erect leader with tiers of lateral branch complexes that give the crown a pagoda shape. Each tier (cf. Fig. 1) consists of  $m$  lateral branch complexes ( $m = 5$  except where otherwise indicated) with a divergence angle,  $\alpha$ , between successively produced complexes. Bifurcations are repeated at every discrete time interval,  $N$ , and take place simultaneously every time. Rule 1 of Fisher and Honda (1977) says that branching increases in discrete units, when the mother axis is  $N$ , the

TABLE 1. Summary of parameters and symbols

$\alpha$ :	angle of lateral branch complex divergence within the tier.
$f$ :	relative flow rate of a branch unit 2 where that of the branch unit 1 (its partner) is 1.0.
$f_1$ and $f_2$ :	the $f$ value of the modified model; $f_1$ = the $f$ value of a pair of branch units 1 and 2 in a main axis (units 1 are components of the main axis); $f_2$ = the $f$ value of a pair of branch units 1 and 2 in side branches.
$m$ :	number of branch complexes in a tier.
$N$ :	discrete time in a computer simulation.
$R_{bh}$ :	Horsfield bifurcation ratio.
$R_{bs}$ :	Strahler bifurcation ratio.
$r_{int}$ :	radius of the interaction circle or column <sup>a</sup> where the length of the first branch unit is unity.
$R_1$ :	ratio of length of a more vigorous branch unit to its mother unit.
$R_2$ :	ratio of length of a less or equally vigorous branch unit to its mother unit.
$\theta_{0i}$ :	angle (in degrees) between the trunk and the first unit of the lateral branch complex.
$\theta_1$ and $\theta_2$ :	branching angles (in degrees) of a more and less vigorous branch unit, respectively; their signs are opposite.

<sup>a</sup> For simplification  $r_{int}$  is assumed to be constant, although in an actual tree its value obviously varies. Similarly the shadow of a leaf cluster is an inverted cone and not a cylinder, for 2-dimensional analysis this can be ignored.

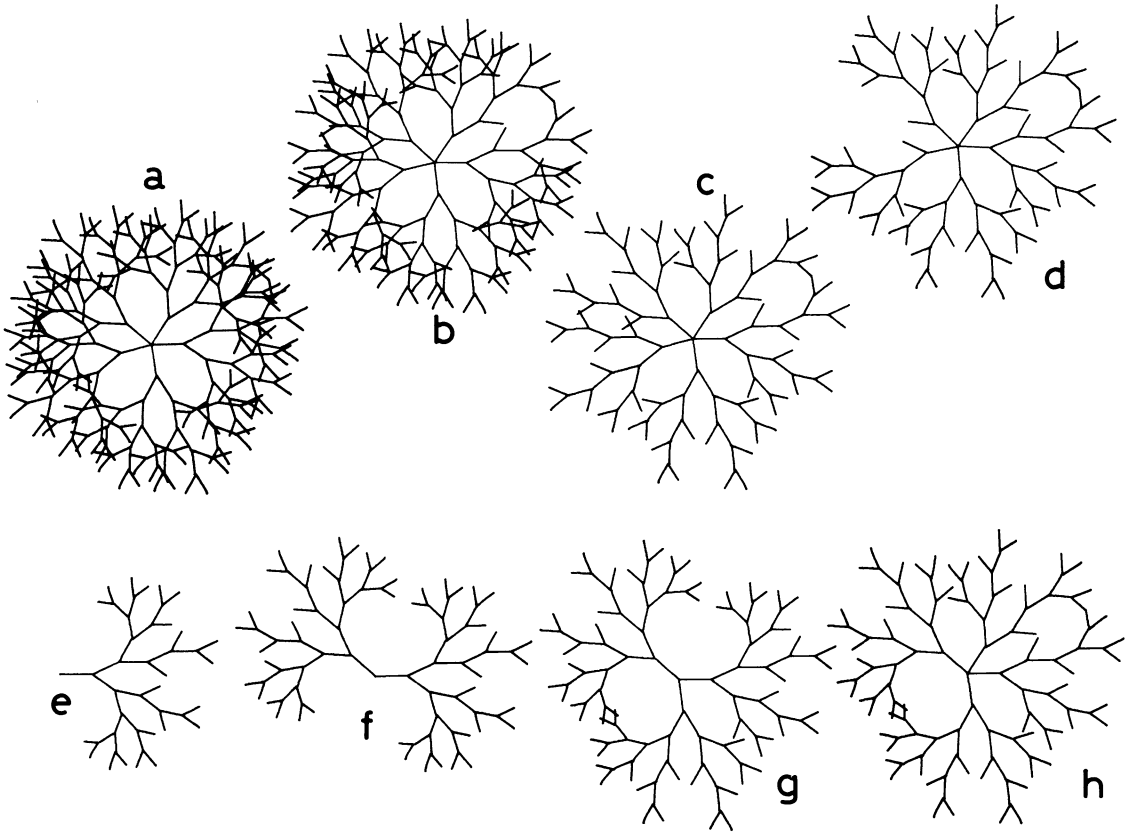


Fig. 3. *Terminalia catappa*, top views of computer simulations of a branch tier with varying degrees of interaction between branches. a–d. Variation with interaction radius  $r_{int}$  = 0 (a), 0.3 (b), 0.5 (c) and 0.7 (d) where  $m = 5$ . e–h and c. Variation with number of lateral branches  $m = 1$  (e), 2 (f), 3 (g), 4 (h) and 5 (c) where  $r_{int} = 0.5$ .

model, some bifurcations will be limited due to an additional rule which accounts for the interaction between branches and which is described below. At each bifurcation two kinds of branches are produced, a more vigorous one (=unit 1) and a less or equally vigorous one (=unit 2) which correspond, respectively, to the branch units in the axils of the third and fifth leaves in the actual branch unit of *T. catappa* (Fisher, 1978). The geometrical relationship between units is determined by two parameters, branch angle ( $\theta_i$ ) and branch length ratio ( $R_i$ ), the length of a daughter branch to that of its mother branch ( $i = 1$  and 2, specifying each kind of branch unit).

The following quantitative values are used for *Terminalia* as before (Honda and Fisher, 1978):  $\theta_1 = 24.4^\circ$ ,  $\theta_2 = -36.9^\circ$ ,  $R_1 = 0.94$ ,  $R_2 = 0.87$  and  $\alpha = 138.5^\circ$ .

**Branch geometry of *Cornus***—*Cornus alternifolia* L. is an understory treelet of the eastern United States. It has the same basic lateral branch geometry as *T. catappa* when consid-

ering branch units 1 and 2 as shown in Fig. 1, but differs in the rhythmic growth of its axes, as described by Hallé, Oldeman, and Tomlinson (1978, p. 172), in relation to the seasonal climate in which it grows. This difference does not affect the simulation of lateral branch complexes. In addition, the first lateral branch forms an angle of  $\theta_{0i}$  with a trunk, but an entire tier is almost horizontal as shown in Fig. 2. The following quantitative values of *C. alternifolia* are derived from averages and ratios of observed values made at Harvard Forest, Massachusetts.  $\theta_1 = 29^\circ$  (sample size, 16),  $\theta_2 = -29^\circ$  (16),  $R_1 = 0.8$  (19),  $R_2 = 0.8$  (9),  $\alpha = 144^\circ$  (10), and  $\theta_{0i} = 51^\circ$  (10),  $m = 5$  is used for a typical tier.

**Interaction between branches in a computer simulation**—*Terminalia catappa* and *Cornus alternifolia* have a leaf cluster at or near the end of every branch unit. When a particular terminal point of a branch unit is close to end points of other branches, its growth and bifurcation may be interfered with. In consid-

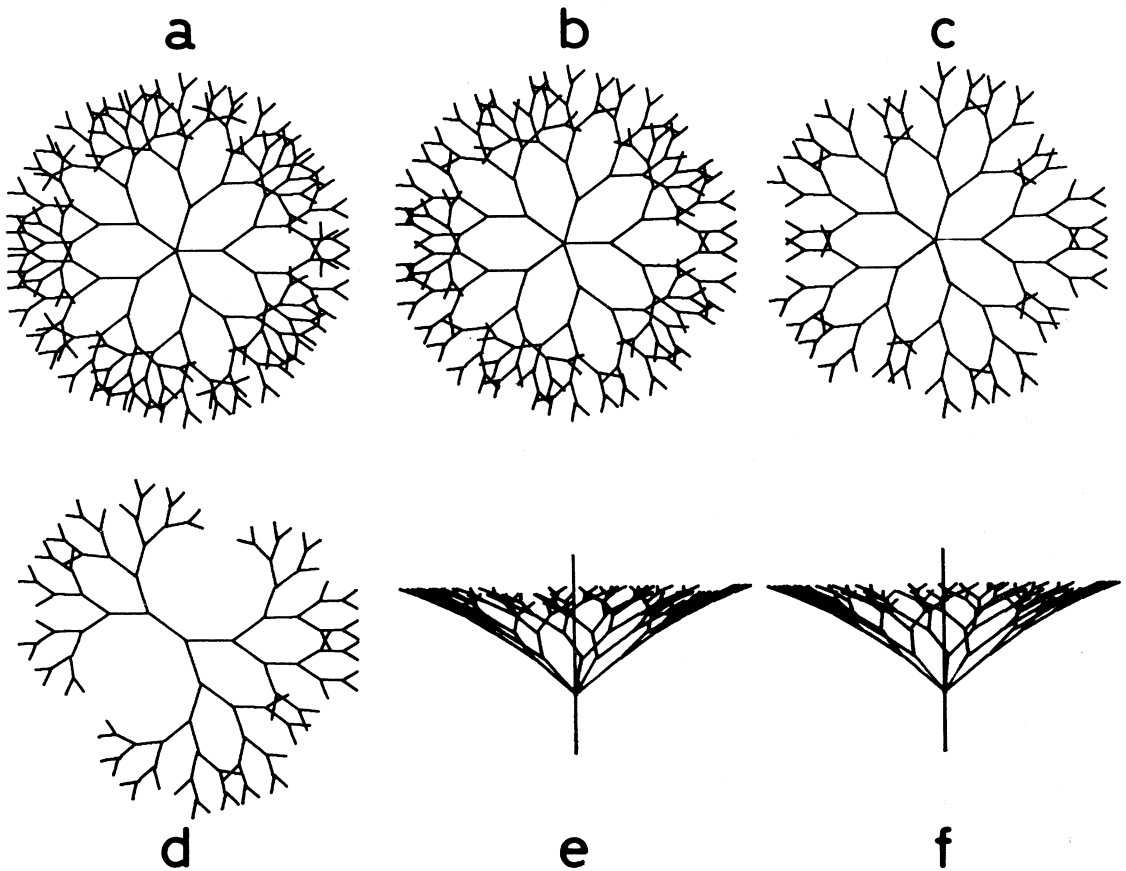


Fig. 4. *Cornus alternifolia*, computer simulation of a branch tier with varying degrees of interaction between branches. a–c. Top views of tiers where  $m = 5$  and  $r_{int} = 0$  (a), 0.2 (b) and 0.3 (c). c and d. Top views of tiers where  $m = 5$  (c) and  $m = 3$  (d) with  $r_{int} = 0.3$ . e and f. Side views of c ( $r_{int} = 0.3$ ,  $m = 5$ ) for stereographic viewing.

ering such an interaction between branches, we will assume a horizontal circle (or a vertical cylinder) whose center is the particular terminal point of a branch. Its radius is  $r_{int}$ , where its first lateral branch (at time  $N = 0$ ) is one unit length. If any end point of another branch occurs inside the circle, and if it is more vigorous than or as equally vigorous as the original terminal point (determined by their  $R_i$  values), the original terminal point does not bifurcate and ceases to grow. Otherwise, it bifurcates according to the rules for branch geometry as noted above.

*Results of computer simulation of branch tiers*—Simulated tiers of *T. catappa* are shown in Fig. 3. When every terminal branch point bifurcates regardless of whether or not its environment is occupied by other branches (i.e.,  $r_{int} = 0$ ), we get the pattern of Fig. 3a. When the terminal point recognizes other end points which are within the distance  $r_{int}$ , there is an inhibition of bifurcation. The results are shown

in Fig. 3b–d with successively increasing  $r_{int} = 0.3, 0.5$  and  $0.7$  for  $m = 5$ . A relatively uniform distribution of branches in the tier is seen in Fig. 3c and d.

Next, the interaction among neighboring lateral branch complexes is examined. When the number of lateral branch complexes with one tier is successively increased,  $m = 1-5$  with  $r_{int} = 0.5$ , the results are shown in Fig. 3e–h and 3c. When  $m \geq 3$ , the distribution of branches is almost as uniform as when  $m = 5$ .

A tier of *C. alternifolia* simulated in the same way as *T. catappa* is shown in Fig. 4 with  $r_{int} = 0, 0.2$ , and  $0.3$  when  $m = 5$  (Fig. 4a–c) and a pattern with  $r_{int} = 0.3$  when  $m = 3$  (Fig. 4d). The side views of Fig. 4c for stereographic viewing are shown in Fig. 4e and f. The first branch unit of all complexes forms an angle ( $\theta_{oi} = 51^\circ$ ) with the vertical leader axis.

*Number of the terminal branches*—The increase of the number of terminal branches during  $N$  in these computer simulations of *T. ca-*

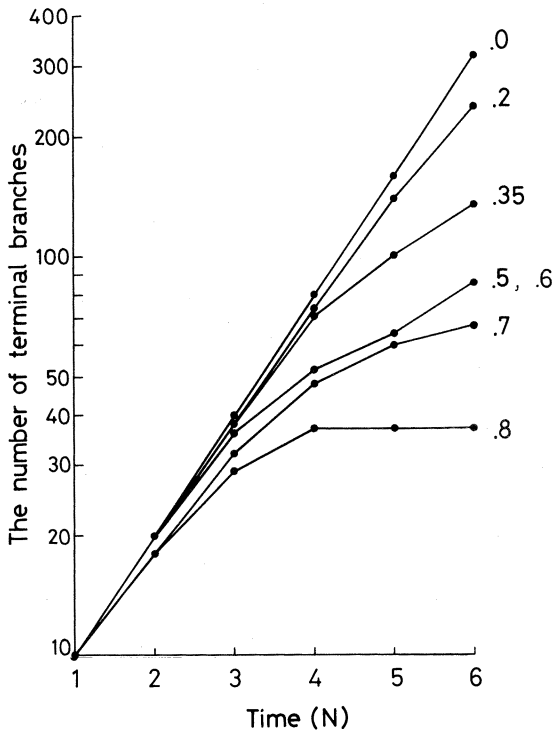


Fig. 5. *Terminalia catappa*, the number of terminal branches in a simulated tier plotted on a logarithmic scale against discrete time  $N$ ; Variation is shown with  $r_{int} = 0.0, 0.2, 0.35, 0.5, 0.6, 0.7$  and  $0.8$  as indicated.

*tappa* is shown in Fig. 5. When  $r_{int} = 0$  the number of terminal branches increases exponentially in proportion to  $2^N$ , so a plot of the logarithm of the number of branches is a straight line. There is an increasing deviation from the straight line as the value of  $r_{int}$  increases from 0.2 to 0.8.

When the interaction among neighboring lateral branch complexes is taken into account, we find that the number of terminal branches increases in the same manner regardless of whether  $m = 3, 4$  or  $5$  when  $N$  is large, as shown in Fig. 6. This is related to the fact that the distribution of branches is similarly uniform when  $m \geq 3$  as shown already in Fig. 3g, h and c.

*Interaction between tiers from different trees*—We have been considering the interaction of branch complexes within a tier. However, interaction among different tiers of one tree and between two or more individual trees can be similarly studied. This approach may be particularly useful in the fields of ecology and forestry. It can also be used for studying the interaction between two reiterated parts of the same crown, i.e., the repetitive develop-

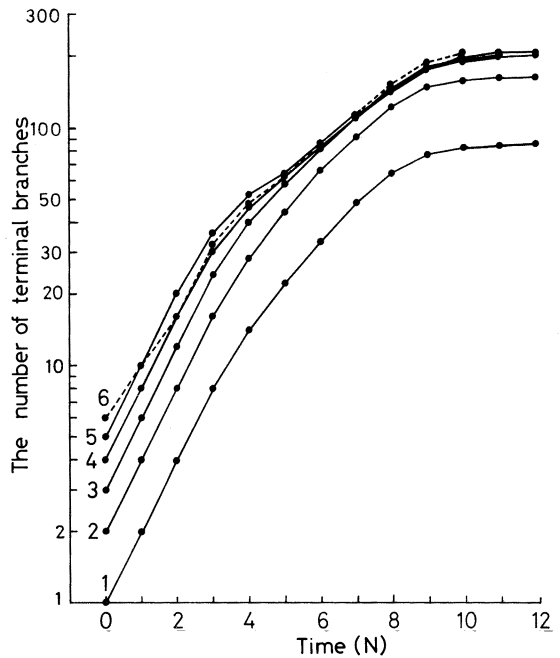


Fig. 6. *Terminalia catappa*, the number of terminal branches in a simulated tier plotted on a logarithmic scale against discrete time  $N$ ; Variation is shown with  $m = 1, 2, 3, 4, 5,$  and  $6$  as indicated.

ment of the sapling form within the crown (see Hallé et al., 1978, p. 269).

Here we will only consider the interaction between two tiers. The centers of two tiers of *T. catappa* are separated by a relative distance of 2.2, where the first lateral branch is one unit in length. The complexes in both tiers begin branching simultaneously at  $N$  and have  $r_{int} = 0.5$ . The resultant pattern at  $N = 5$  is shown in Fig. 7, above. The respective patterns of the two individual tiers are shown separately in Fig. 7, below. Further numerical analysis has not been attempted, but the methods are available as outlined above.

**DIFFERENT FLOW-RATES—*Terminalia* and *Tabernaemontana* models**—The same basic model used in the study of branch interaction in *Terminalia catappa* was used, with consideration only given to patterns spread in one plane. As before, the set of branch parameters used in the model were:  $\theta_1 = 24.4^\circ, \theta_2 = -36.9^\circ, R_1 = 0.94,$  and  $R_2 = 0.87$  (from Honda and Fisher, 1978). In addition, a second model, based on a specimen of *Tabernaemontana* sp., cultivated at Fairchild Tropical Garden (Miami), was used. In this species, growth of the branch complex is sympodial by substitution (Hallé et al., 1978), rather than sympodial by apposition, with each unit in the com-

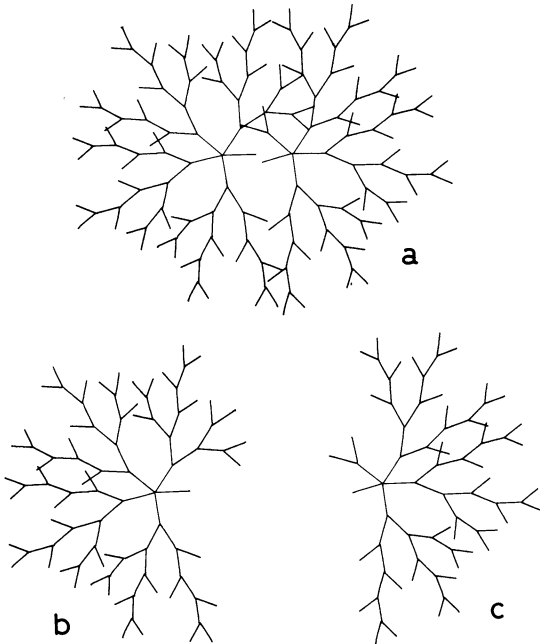


Fig. 7. *Terminalia catappa*, interaction between two separate but juxtaposed tiers in a computer simulation where  $r_{int} = 0.5$ . Distance between the centers of the two tiers is 2.2 where the first lateral branch is one unit in length. Above (a), the computer simulation; below (b, c), the two individual tiers represented separately, to show the extent of branch loss in each tier as a result of interaction.

plex determinate by parenchymatization of its apex. This distinctive morphogenetic pattern is not important in the actual modelling process. For *Tabernaemontana* the branch parameters used in the model were:  $\theta_1 = 29^\circ$  (sample size = 17),  $\theta_2 = -54^\circ$  (17),  $R_1 = 0.99$  (19), and  $R_2 = 0.85$  (14).

To the basic branching models mentioned above, we have added a new branching rule which restricts bifurcation. In an actual tree every terminal branch does not bifurcate, that is, frequency of bifurcation is different at each terminal branch unit. The mechanism that determines this frequency is not known, but, presumably, is determined by the morphogenetic status of the meristem and its position in the complex. In the following model, the difference of frequency of bifurcation is attributed to a difference of "flow rate" of some hypothetical material. In the simplest terms, this material could be an unidentified substance or nutrient that is a determiner for the growth and branching of units. In an actual tree, the situation is obviously more complex. The rationale for such a hypothesis is elaborated in the discussion. The amount of the material trans-

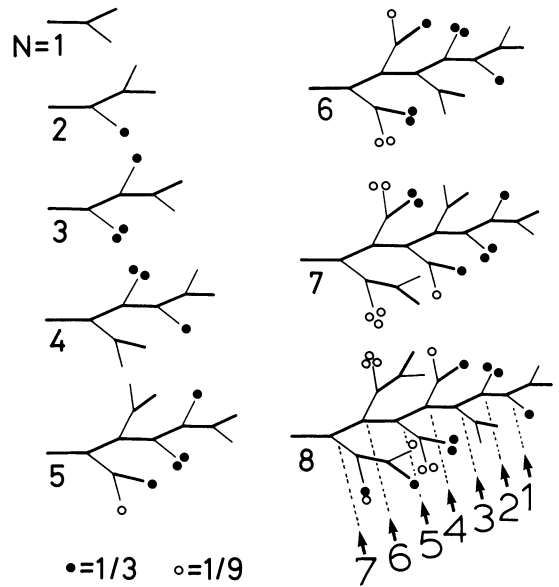


Fig. 8. Diagrams of the branching model with different flow rates. In this example,  $f = 1/3$ . During the discrete time  $N = 1$ , the amount 1.0 and  $1/3$  of material required for branching accumulates at the end points of terminal branch units 1 (thick line) and 2 (thin line), respectively. Since the necessary critical amount for branching is 1.0, unit 1 bifurcates and unit 2, which has the amount  $1/3$  (●) at its end point, remains unchanged. Unit 2 accumulates the amount  $2/3$  (●●) at  $N = 3$ , and the amount 1.0 ( $= 3/3$ ) at  $N = 4$  when it bifurcates. During  $N = 5$  these daughter branch units 1 and 2 accumulate the amount  $1/3$  (●) and  $1/9$  or  $1/3 \times 1/3$  (○) because their mother branch's  $f = 1/3$ . Arrows indicate organization of the distal part of a branch complex (or its mirror image) at discrete times:  $N = 7, 6, 5 \dots$  etc.

ported through a less vigorous branch unit 2 in a certain time is  $f$ , the relative flow rate. This is some fraction of the amount (set at 1.0) transported through the branch unit 1, the more vigorous partner of the unit 2. Usually  $f$  is less than 1.0 because branch unit 1 is generally more vigorous than a unit 2. Initially,  $f$  is assumed to be constant throughout the branch complex; its variation within the complex will be considered later in the present report. The material accumulates at the end point of a terminal branch. The critical amount 1.0 of the material is assumed to be necessary to permit subsequent bifurcation.

An example in which  $f = 1/3$  is shown in Fig. 8. There is a pair of branch units at  $N = 1$ . The material accumulates at both end points until  $N = 2$ . At  $N = 2$ , unit 1 has accumulated the amount 1.0 and bifurcates, whereas unit 2 has only the amount  $1/3$  and remains as a single unit. Unit 2 does not bifurcate during three discrete steps or units of time. At  $N = 4$ , unit 2 has accumulated the amount 1.0

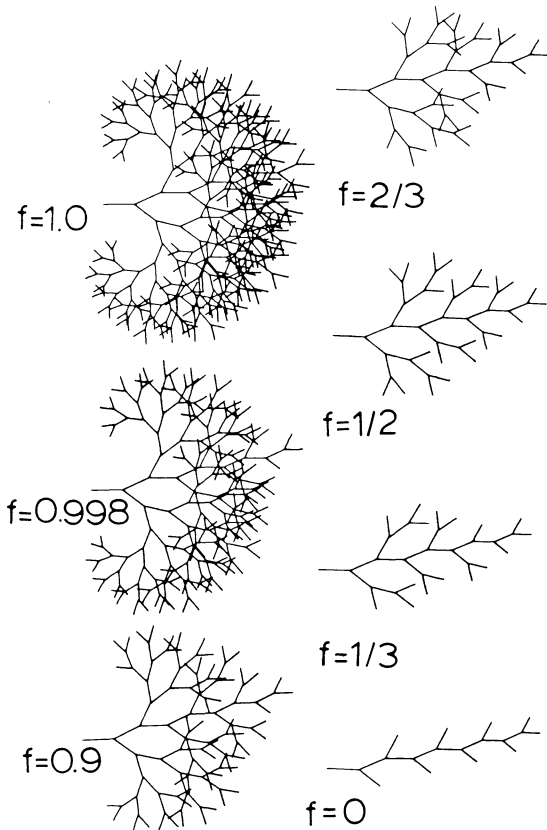


Fig. 9. Branching patterns using different values of  $f$  at  $N = 8$ . The values of  $T. catappa$  are used for the parameters of branching  $R_1, \theta_1$  ( $i = 1, 2$ ).

$(\frac{1}{3} + \frac{1}{3} + \frac{1}{3})$  and bifurcates. Figure 8 itself may be self-explanatory, but we will add a few notes here.

When a pair of branch units has its unit 2 in a proximal chain of branch units, the flow rate through the pair is reduced by  $f$ , that is, the relative flow rates of units 1 and 2 in a pair are  $f$  and  $f \times f$ , respectively. This effect is first seen at  $N = 5$  in Fig. 8, where closed circles represent  $\frac{1}{3}$  and open circles  $\frac{1}{9}$  of the critical amount.

The ratio of  $f$  is a value only for a pair of terminal branch units. After several discrete times, the flow rate of a branch unit varies depending on how many branch units it has distal to itself in the branch complex. The more distal branch units it has, the more material it should necessarily transport.

A characteristic of the branch pattern determined by our model is that the distal part of a complex has the same pattern as the entire complex at an earlier time. For example, the distal parts of the pattern of  $N = 8$  in Fig. 8, which are shown beyond each of the arrows, are the same as, or the mirror image of,  $N =$

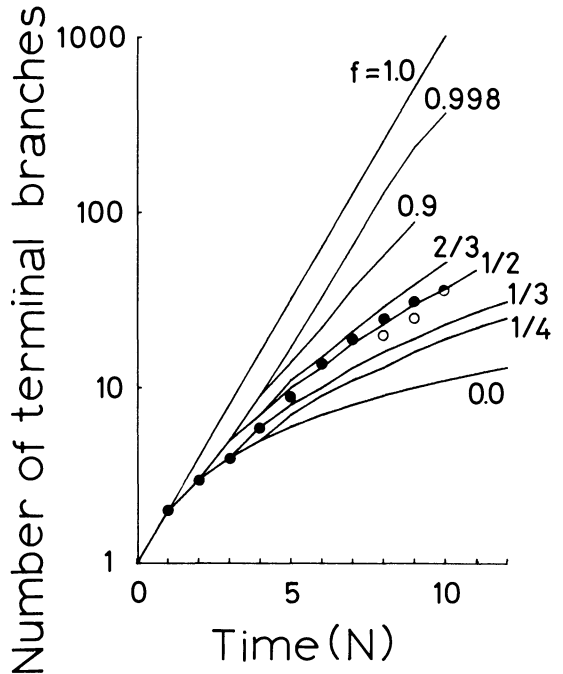


Fig. 10. The number of terminal branches for the patterns in Fig. 9 plotted on a logarithmic scale against discrete time  $N$ . Respective  $f$  values are indicated. ●, ○, ◐: actual number of terminal branches observed in *Tabernaemontana* sp., as explained in detail in the text.

7, 6, . . . , 1. This property becomes useful in subsequent analysis.

*Results of different flow rates*—Simulated branching patterns with various values of  $f$  are shown in Fig. 9, and numbers of terminal branches of these and additional patterns are listed in Table 2 and plotted in Fig. 10.

When  $f = 1.0$ , that is, a branch unit 2 has the same flow rate as a branch unit 1, all end points of terminal branches bifurcate. The branching pattern is very complicated (Fig. 9,  $f = 1$ ), and the number of terminal branches increases exponentially (Table 2 and Fig. 10). As the value of  $f$  decreases, that is, unit 2 transports material more slowly than unit 1, the overlap of branches decreases and a main axis which shows a zigzag pattern becomes recognizable (Fig. 9, from  $f = 1$  to 0). When  $f = 0$ , unit 2 never bifurcates, and we get the simplest pattern (Fig. 9,  $f = 0$ ).

We have assumed that the  $f$  value is the same in every pair of branch units. We can now examine the case of different  $f$  values in certain locations of a branch complex. In some branch complexes a main axis, which is thick and zigzag, is very distinct and can easily be distinguished from other parts (side branches) of the

TABLE 2. Number of terminal branches in simulations of branching patterns<sup>a</sup>

f	Discrete time (N)												
	0	1	2	3	4	5	6	7	8	9	10	11	12
1.0	1	2	4	8	16	32	64	128	256	512			
0.998	1	2	3	5	9	17	33	65	129	235	368		
0.98	1	2	3	5	9	17	32	50	82	146	266	431	
0.9	1	2	3	5	9	14	22	37	57	88			
3/4	1	2	3	5	8	12	18	26	37	52			
2/3	1	2	3	5	7	11	15	21	29	39	52		
1/2	1	2	3	5	7	10	13	18	23	30	37	47	
2/5	1	2	3	4	6	8	10	13	16	20	25	30	36
1/3	1	2	3	4	6	8	10	13	16	19	23	27	31
1/4	1	2	3	4	5	7	9	11	13	16	19	22	25
0.0	1	2	3	4	5	6	7	8	9	10	11	12	13

<sup>a</sup> Some of these patterns are illustrated in Fig. 9 and 10.

branch complex. Bifurcations which take place directly from a main axis are assumed to be different from other bifurcations, and their  $f$  value is defined as  $f_1$ . Thus, the ratio of flow rate of branch unit 2 to that of unit 1 (the main axis consists only of units 1) is  $f_1$ . The  $f$  value of other bifurcations, which are bifurcations in side branches, is  $f_2$ . The case of  $f_1 = f_2 (= f)$  is the original branching model with different flows as mentioned previously.

The difference in branching patterns with  $f_2$  being varied and  $f_1$  fixed at 1.0 is shown in Fig. 11a–f. These branch complexes are wider than similar ones shown in Fig. 9. Next,  $f_1$  is varied while  $f_2$  is fixed at  $1/2$ , and the results are shown in Fig. 11d and g–j. The width of the branch complexes is shortened, and side branches disappear in the extreme case of a small  $f_1$  value ( $f_1 = 0.1$ , Fig. 11j).

Modification of the branching model also affects the number of terminal branches. Figure 12a shows a decrease in number of branches as  $f_2$  values decrease while  $f_1$  is fixed at 1.0. As  $f_1$  values decrease, similar changes occur in Fig. 12b–d, when  $f_2$  is fixed at  $1/2$ ,  $1/3$  and 0.0. Patterns of Fig. 11d and 11g–j correspond to Fig. 12b. Some of the patterns corresponding to Fig. 12c and d are not represented. However, we can represent them: for example, by decreasing the width of Fig. 11f, similar to the way that Fig. 11d was made narrower to become Fig. 11g–j, we can get the patterns that correspond to those of Fig. 12d.

*Similarity of the model to real branches*—We will now compare real tree branches to computer simulations using the branching model with different flow rates. A close fit should give us a reasonable approximation of the  $f$  value of the real branch, if in fact this hypothetical flow principle is operative. Se-

lected lateral branches from two species are used in this preliminary examination.

*Tabernaemontana* sp: A representative lateral branch complex from this species viewed from above is drawn in Fig. 13b. The real branch pattern is compared with the theoretical patterns using  $f = 1/2$  and  $1/3$ . The theoretical pattern with  $f = 1/2$  (Fig. 13c) is quite close to the real pattern.

In the distal parts of the real branch we can distinguish green, greenish brown, and brown parts representing successive age differences. The number of terminal branches that were produced most recently can be determined by counting the green parts. Similarly, we can count the number of terminal branches of the previous growth stage by noting greenish brown parts, and the number of those of the stage before by noting brown parts. The results are 36, 25, and 20 respectively, and are indicated in Fig. 10 and 12 by the open and half-closed circles.

We have another way to determine indirectly the number of terminal branches of previous stages. As mentioned above, the theoretical branch pattern contains its younger pattern in its distal part. If we assume a real branching pattern has been made according to the branching model with different flow rates, we can estimate its younger patterns. Using this approach, we obtain the following series of the number of terminal branches from a real pattern as in Fig. 13b: 36, 31, 25, 19, 14, 9, 6, 4, 3, 2, and 1. These data are indicated by the closed and half-closed circles in Fig. 10 which are close to the curves of  $f = 1/2$  and  $1/3$ . The real branching pattern is close to the pattern of  $f = 1/3$  at the young stages and to the pattern of  $f = 1/2$  at the older stages. The real branch is also compared with the modified model with

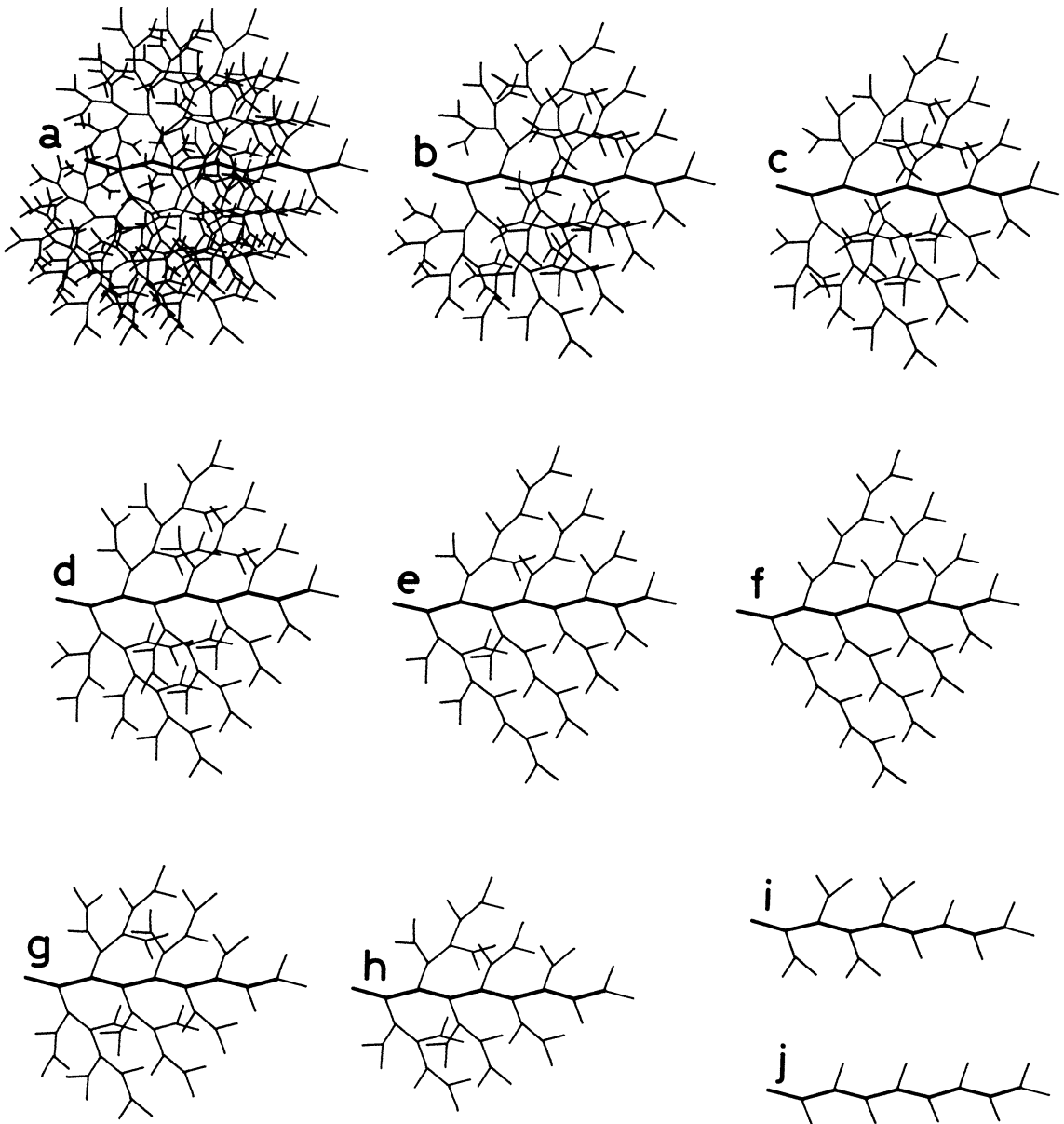


Fig. 11. Variation of a branching pattern with the values of  $f_1$  and  $f_2$ . a-f.  $f_2 = 1.0$  (a), 0.9 (b),  $\frac{2}{3}$  (c),  $\frac{1}{2}$  (d),  $\frac{1}{4}$  (e), 0.0 (f) where  $f_1 = 1.0$ . d and g-j.  $f_1 = 1.0$  (d), 0.9 (g),  $\frac{3}{4}$  (h),  $\frac{1}{4}$  (i) and 0.1 (j) where  $f_2 = \frac{1}{2}$ . The values of *Tabernaemontana* are used for the parameters of branching:  $R_1, \theta_i$  ( $i = 1, 2$ ).

$f_1$  and  $f_2$ . Using the modified model, the patterns close to the real one occur when  $f_1$  and  $f_2$  are also around  $\frac{1}{2}$  and  $\frac{1}{3}$  (closed and half-closed circles in Fig. 12).

*Terminalia catappa*: A representative lateral branch complex of this species is compared with patterns of the model using  $f = \frac{1}{2}$  and  $\frac{1}{3}$  (Fig. 14). Theoretical patterns of these models are not very different from the real one.

However, another larger, and more highly branched complex of *T. catappa* is not closely simulated by the theoretical one as shown in Fig. 15a. The first side branch (arrow) of the theoretical pattern is too small in comparison with the real one. If we add another assumption to the theoretical model that the  $f$  value of the first branching is 1.0 whereas the  $f$  value of the following branching is smaller than 1.0 (for example  $f = 1/3$ ), the real branch is more

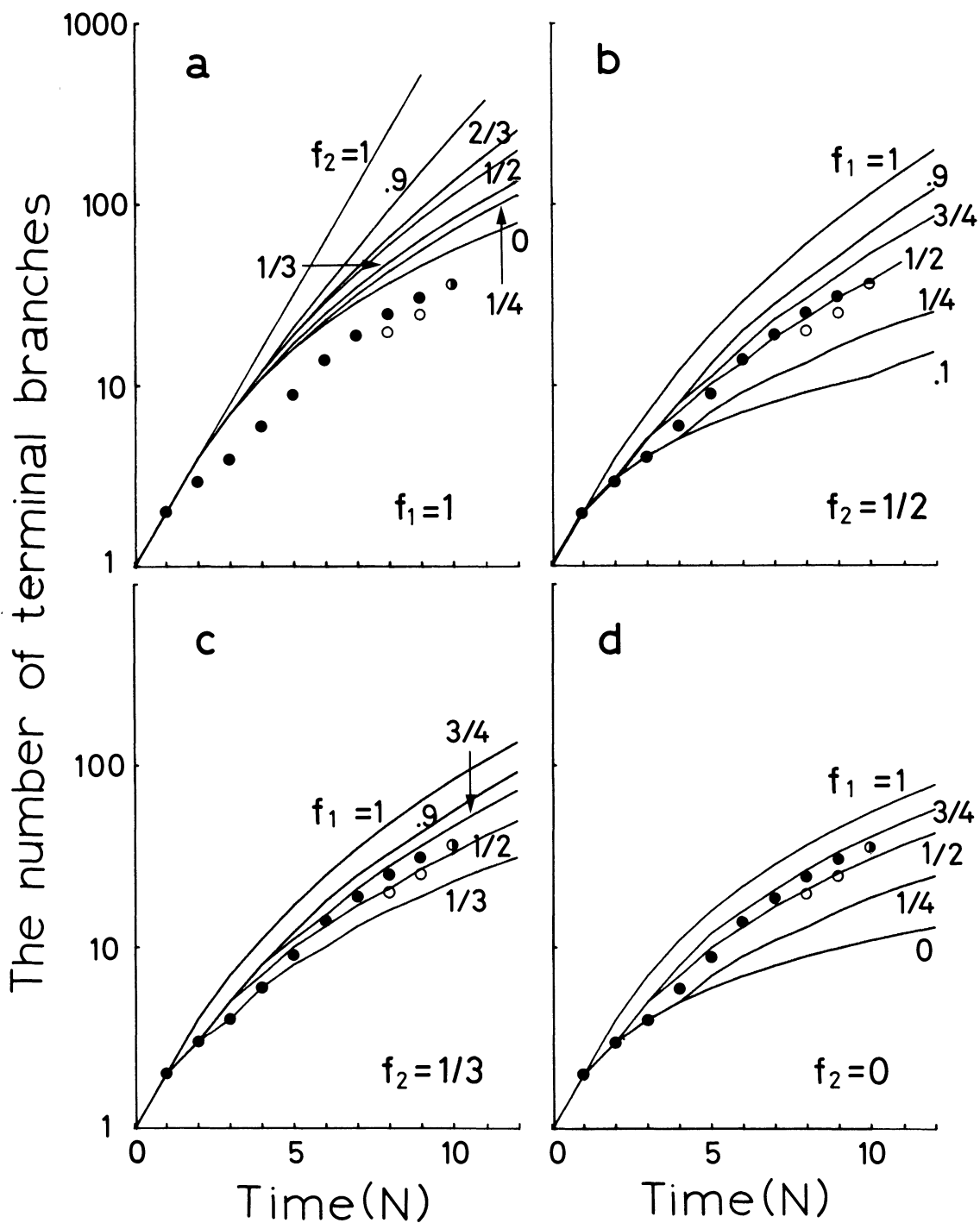


Fig. 12. The number of terminal branches plotted on a logarithmic scale against discrete time  $N$ . a. Variation with  $f_2$  where  $f_1 = 1.0$ . b-d. Variation with  $f_1$  where  $f_2 = 1/2$  (b),  $1/3$  (c) and 0.0 (d). ●, ○, ◐, : actual values; See the legend of Fig. 10.

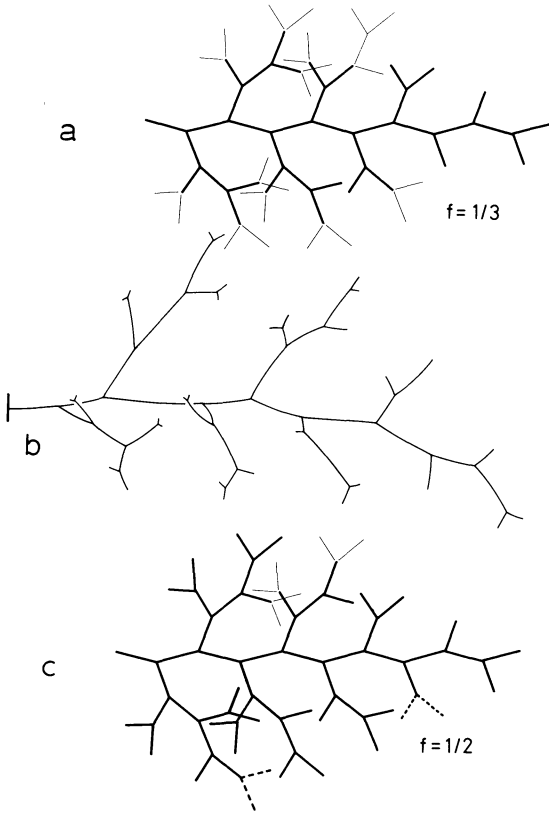


Fig. 13. Comparison of a real lateral branch complex and theoretical patterns from the branching model with different flow rates. **a** and **c**. Thick solid and broken lines represent theoretical patterns of  $f = 1/3$  (**a**) and  $1/2$  (**c**). Thin lines indicate the real branches which are not included in theoretical patterns. Thick broken lines indicate theoretical branches which are not included in the real pattern. **b**. Top view of the real pattern of a lateral branch of *Tabernaemontana* sp. One side branch, which is the most proximal, is omitted from the figure, but the number of terminal branches was counted using the entire branch complex.

closely simulated by the theoretical model (Fig. 15b). This assumption is reasonable because the first fork of a lateral branch complex is usually equal, while in later forks, there is typically a difference of vigor between a pair of daughter units (Fisher, 1978).

**BIFURCATION RATIOS—Branch interaction—**From the computer simulations of trees, we have determined both bifurcation ratios and the number of terminal branch units (Strahler, 1964; Tomlinson, 1978). Since this information is easily extracted and allows comparisons to be made on a quantitative basis some explanation of the analytical principles is necessary since two different methods are used.

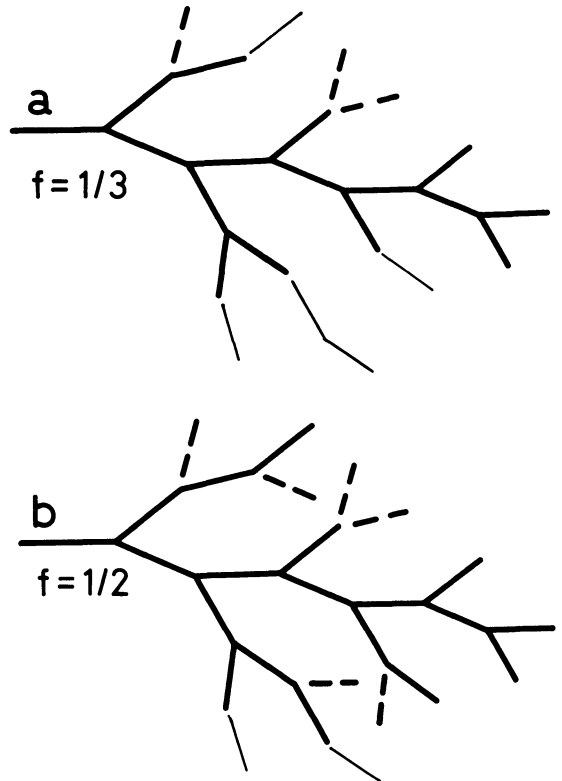


Fig. 14. Comparison of a real lateral branch complex and theoretical patterns from the branching model with different flow rates. Thick solid and thin lines together indicate a real lateral branch of *T. catappa*. Thick solid and broken lines together indicate theoretical patterns with  $f = 1/3$  (**a**) and  $1/2$  (**b**).

In the Strahler bifurcation ratio ( $R_{bs}$ ) the terminal branches are designated order 1, and two of these meet to form an order 2 branch, and so on down to the trunk. When two branches of different orders meet, the conjoined branch takes the highest order number. That is, the union of an order  $i$  and order  $j$  branch is assigned order  $i + 1$  when  $i = j$ , or order  $\max(i, j)$  when  $i \neq j$ . Finally, any two or more contiguous branches of the same order are considered to constitute only one branch. The analysis of a real tree is best made by destructive sampling, eliminating all branches of the same order at each successive step. The computer was programmed to carry out these steps in simulated trees.

The number of branches in each order when plotted on a logarithmic scale against order number commonly gives a linear plot. The slope of this line is determined by a least squares fit, and the antilog of the absolute value of the slope is the  $R_{bs}$  (e.g., Strahler, 1964).

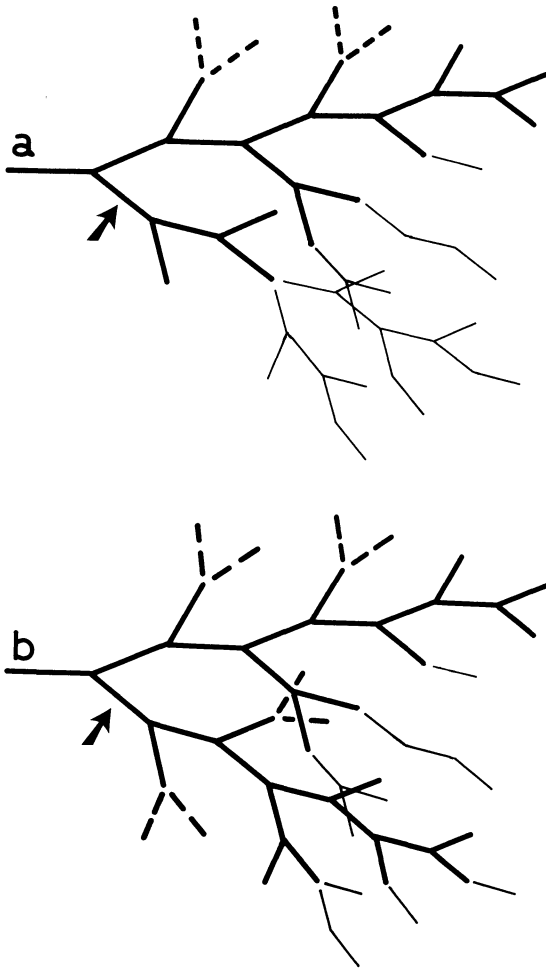


Fig. 15. Comparison of a real lateral branch complex and theoretical patterns by the branching model with different flow rates. Thick solid and thin lines indicate a real lateral branch of *T. catappa*. Thick solid and broken lines indicate theoretical patterns with  $f = 1/3$ . a. According to the original model with different flow rates. b. According to the modified model in which the  $f$  value of the first branching only (arrow) is 1.0.

The bifurcation ratio has been considered to have ecological significance (Whitney, 1976), but there may be a wide range of values in a given species (Oohata and Shidei, 1971; Steingraeber, Kascht, and Frank, 1979). Our theoretical results shed some light on the actual significance and usefulness of bifurcation ratios.

The Horsfield bifurcation ratio ( $R_{bH}$ ) is the same as Strahler's except that a slightly different ordering system is used leading to different values. The mother branch is numbered one order higher than the higher-ordered

daughter branch. That is, the union of an order  $i$  and order  $j$  branch is always assigned order  $\max(i, j) + 1$  (Horsfield, 1967). Results of both methods of analysis are presented because Strahler ordering has been used exclusively in the analysis of botanical trees in the papers cited above. However, Horsfield analysis makes the most comprehensible comparison within a series of simulations where only one parameter is varied.

*Bifurcation ratios in simulated trees*—The resultant branching patterns of tiers are analyzed by both the Strahler and Horsfield methods of ordering. Using these two methods, the number of branches in each order is plotted logarithmically against order number (Fig. 16a and b), and both bifurcation ratios,  $R_{bS}$  and  $R_{bH}$ , are obtained (Fig. 17a and b, broken lines).

Variation of bifurcation ratios with  $r_{int}$  is shown in Fig. 17. When  $r_{int} = 0$ ,  $R_{bS}$  and  $R_{bH} = 2.0$  and remain constant during discrete time in computer simulation. However, they deviate increasingly from 2.0 as  $r_{int}$  increases. It should be noted that the bifurcation ratios vary irregularly with  $N$  (Fig. 17a and b).

Variation of bifurcation ratios with the number of lateral branch complexes ( $m$ ) is shown in Fig. 18a and b. When  $m$  becomes large, that is, the region of interaction between adjacent complexes becomes large, the bifurcation ratios deviate from the value 2.0. These results show that within the constraints imposed by our simple rules, bifurcation ratios are not a fixed property of trees. They change with different stages of growth ( $N$ ) and with degree of branch crowding ( $m$ ).

*Actual measurement of bifurcation ratios*—Strahler bifurcation ratios were calculated from measurements of real *T. catappa* trees. Branch tiers with several  $m$  values were selected. The individual branch complexes in each tier often had differing  $N$  values. The average  $N$  value for real tiers are noted in Fig. 16a (dotted lines). A variety of real  $R_{bS}$  values for tiers with different  $m$  values are given in Fig. 18a (open circles). In the case of the Horsfield bifurcation ratio, we have two possible ways of ordering because *Terminalia*-branching sometimes shows unforked (nonbifurcating) branching in which only one branch grows out (Fisher, 1978), e.g., a mother branch unit has only one daughter branch unit whose order is  $j$ . There are two possible methods for ordering the mother unit; the mother unit can be either  $j$  or  $j + 1$ . It is not at all clear which of the two

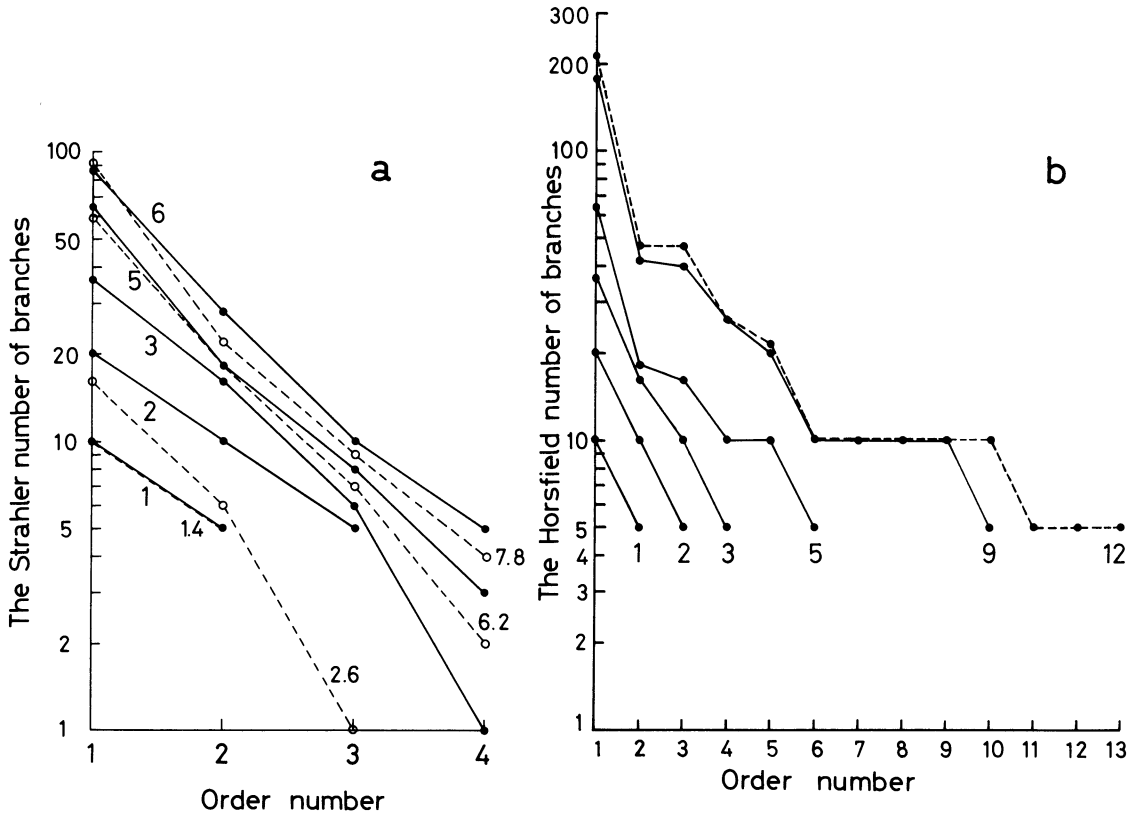


Fig. 16. *Terminalia catappa*. a. Strahler number of branches in each order from computer simulations ( $r_{nt} = 0.5$ , solid lines) and actual observations (broken lines) of tiers with  $m = 5$  plotted against order number. Discrete times in computer simulations indicated by integers to the left. Nonintegers to the right refer to average values of  $N$  calculated from observed tiers. These are nonintegers because not all complexes within a real tier grow at the same time. b. The same computer simulations analyzed with the Horsfield number of branches. Numerals show the discrete times in computer simulations.

ordering methods is more appropriate. Therefore, we will not indicate the Horsfield bifurcation ratio of real trees in the present paper.

Strahler bifurcation ratios of real trees of *T. catappa* are shown in Fig. 18a (open circles). We cannot definitely compare these theoretical and observed data at present since we have relatively few observations. In addition, the computer simulations do not describe unforked branching in which only one branch grows out as it sometimes does in actual *Terminalia*-branching (Fisher, 1978). However, we should notice a similarity of variation between theoretical and observed Strahler bifurcation ratios. For example, Fig. 18a shows that the theoretical curve of  $m = 5$  shows a sudden increase around  $N = 3$  and 4 and decreases again, and the observed values with  $m = 5$  is large over the range,  $N = 2-6$ .

*Differing flow rates*—The Strahler and Horsfield numbers of branches for each branch or-

der are plotted logarithmically against order (examples with  $f = \frac{1}{2}$  shown in Fig. 19a and b). Both bifurcation ratios,  $R_{bs}$  and  $R_{bh}$ , are obtained for every discrete time unit in simulations and are shown in Fig. 20a and b.

The Strahler and Horsfield bifurcation ratios for patterns shown in Fig. 11 were determined. Figure 21a and b shows the case of variation in  $f_2$  values when  $f_1$  is fixed at 1.0. Figure 21c and d shows the case of variations in  $f_1$  values when  $f_2$  is fixed at  $\frac{1}{2}$ . These ratios are similar to those shown in Fig. 20.

**DISCUSSION**—The present paper is intended as an approach to questions of factors limiting branch multiplication in trees. In the first factor taken into consideration, the "environmental factor," nearness of neighboring terminal units, influences branching capability. In the second, an endogenous factor involving the relative capacity for further development of twin axes is considered.

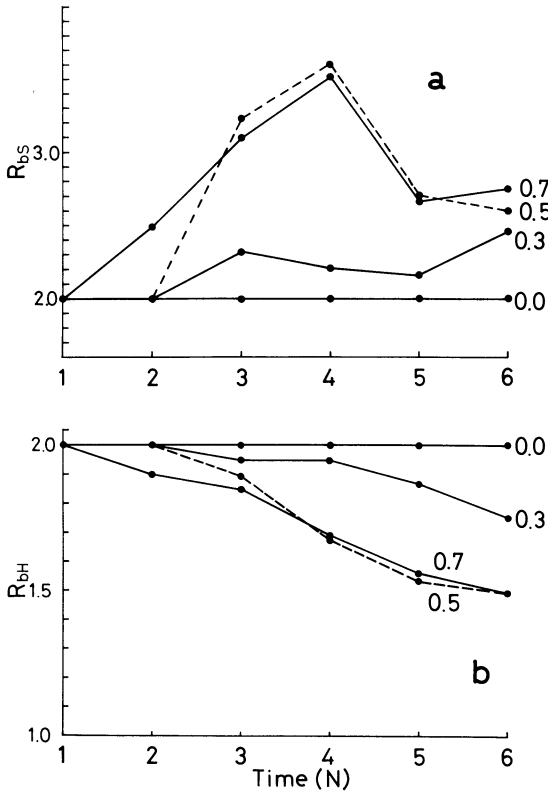


Fig. 17. *Terminalia catappa*, variation of the Strahler (a) and Horsfield (b) bifurcation ratio with  $r_{int}$ . Each kind of bifurcation ratio is plotted against discrete time in computer simulations of a single tier ( $m = 5$ ). The values of  $r_{int}$  from 0.0 to 0.7 are indicated. Broken lines ( $r_{int} = 0.5$ ) are ratios derived from Fig. 16a and b.

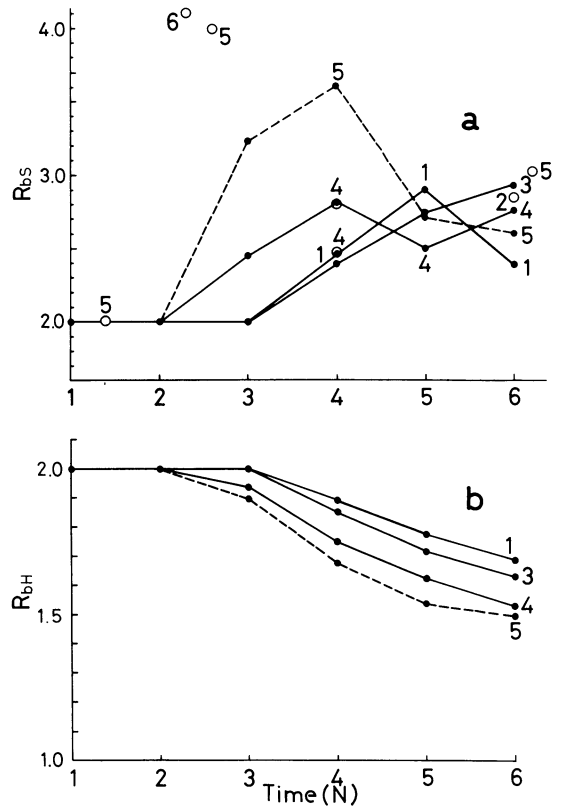


Fig. 18. *Terminalia catappa*, variation of the Strahler (a) and Horsfield (b) bifurcation ratio with  $m$ . Each kind of bifurcation ratio (solid circle) is plotted against discrete time in computer simulations of a tier ( $r_{int} = 0.5$ ). Some observed values from actual trees are shown by open circles. The values of  $m$  from 1 to 5 are indicated.

**Branch interaction**—The use of the concept of “circle of inhibition” can be justified as a result of shading effects (since in the examples used each end point is occupied by a rosette of leaves) together with physical damage where leaves and particularly buds make mechanical contact. Feedback mechanisms in terms of nutrient and growth substance supply, as discussed below, could be the actual regulatory mechanism.

We ourselves have made relatively few observations of the number of terminal branches and of the bifurcation ratios that correspond to the present computer simulations. Some of our observed data of bifurcation ratios of real *T. catappa* trees have been presented for comparison with the theoretical values. Measurements on *Rhus typhina* of actual number of shoots at different ages (data of J. White cited in fig. 30 by Hallé et al., 1978) show a decline due to a loss of branches, so that the exponential rate of increase of terminal branches is less than two. This species has a three-di-

dimensional pattern in the crown, whereas our essentially independent branch tiers are two-dimensional. More information is available for shoot systems of herbaceous plants (White,

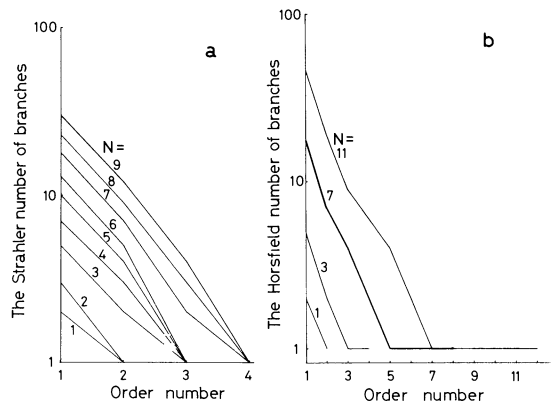


Fig. 19. The Strahler (a) and Horsfield (b) number of branches plotted on a logarithmic scale against order for simulations using  $f = 1/2$ . Discrete times are indicated by numerals.

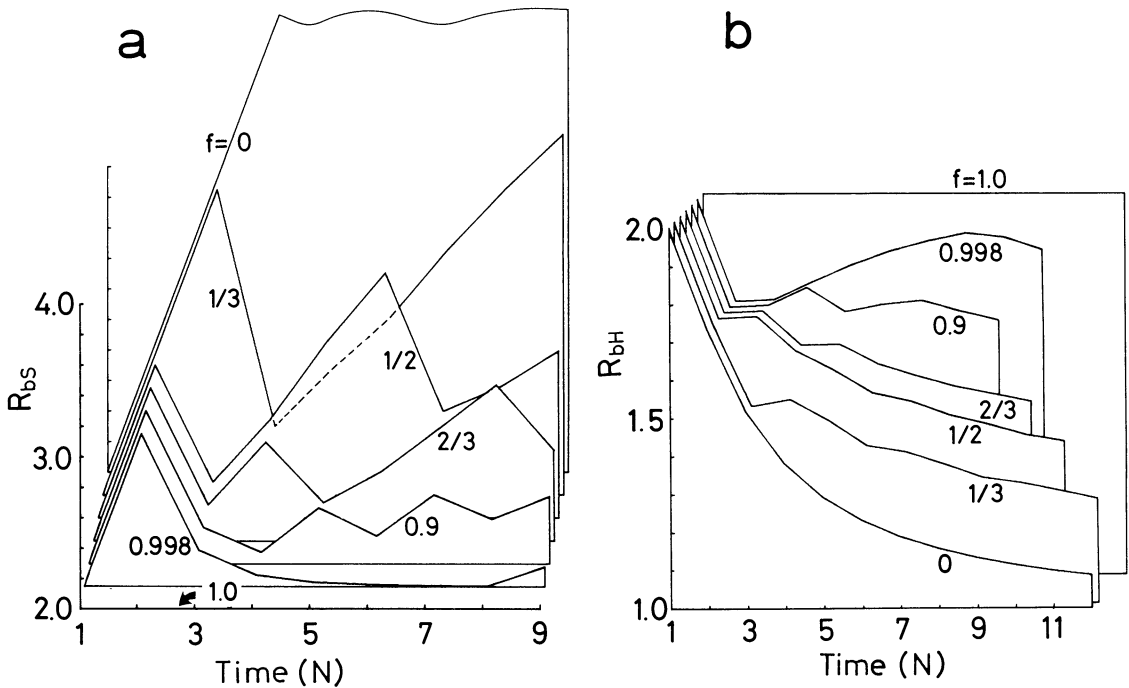


Fig. 20. The Strahler (a) and Horsfield (b) bifurcation ratios against discrete time for simulations using different values of  $f$  as indicated.

1979; Bell and Tomlinson, 1980). Although the computer simulations illustrated here are very simple, we hope that they might help in planning observations and measurements of actual trees.

The present simulation model involves several simple assumptions. The process of branching (or bifurcation) in the computer simulation is discrete in time. Only those terminal branch units which, at a given unit of time, do not have any neighboring branch end points within a circle of radius  $r_{int}$  bifurcate. After bifurcation some of the resulting terminal branches will then interact. This interference is neither measured nor effective until the next discrete time unit. This assumption reflects the simplicity of the computer program, but may be reasonable physiologically since both bifurcation and growth of branches uses nutrients which have been synthesized and/or translocated during the previous discrete time stage. When leaf clusters of neighboring terminal branches overlap to a significant degree, there could be insufficient nutrients for the next flush of branches. On the other hand, mechanical interaction and possible physical damage could occur continuously during discrete time intervals.

Only a branch tier, instead of a total tree, is simulated in a computer. This is a reasonable simplification of the canopy geometry because

every branch tier is separate vertically along the leader axis and can be regarded as an independent foliage layer.

In determining the competition between branches in the simulation, we have considered only the abortion of young branch units to simplify the computer program. Abscission of old branch units and the resulting release of competition should be included in future simulation studies.

*Different flow rates*—In the second study, we have shown that only one intrinsic factor, difference in bifurcation rates of daughter branches based on different rates of flow in the products of a previous bifurcation, can likewise result in realistic simulations.

The model assumes that there is a hypothetical material which flows through branches and accumulates up to a critical threshold above which bifurcation takes place. Such material might be carbohydrates, a regulating substance like a mineral or hormone, water which could affect photosynthesis and meristem activity, or a combination of these. In any case, an innate physiological difference (as seen in flow rate) between two branches is presumed. Such a difference does in fact produce complex branching patterns that are similar to those found in real trees. We therefore present theoretical evidence that the on-

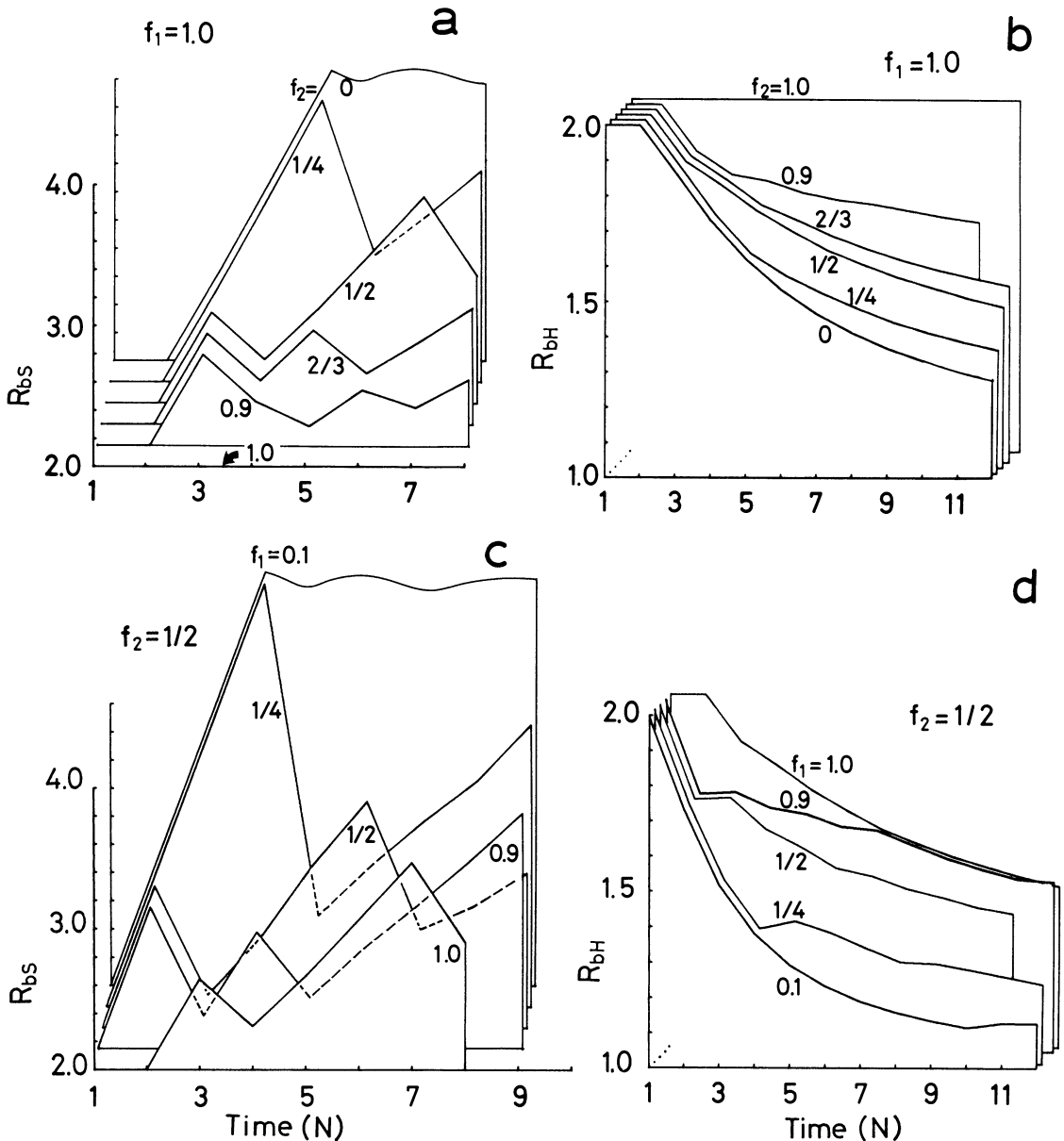


Fig. 21. The Strahler (a,c) and Horsfield (b,d) bifurcation ratio against discrete time for simulations using various  $f_1$  and  $f_2$  values. a,b. Variation with  $f_2$  where  $f_1 = 1.0$ . c,d. Variation with  $f_1$  where  $f_2 = 1/2$ .

togeny of patterns can be conceptualized in terms of acropetal movement and accumulation of materials toward the distal meristems, similar to a "nutritional control" of branching and apical dominance (Phillips, 1975). Although a true dichotomy or bifurcation of the apex is not involved in the species we have examined nor is part of our model, the model of apical bifurcation presented by Thornley (1977) has a bearing on our model. Thornley developed a very simple model, based on the relative sizes of the two daughter apices, which

can generate a wide variety of tree-like patterns. The apex will only divide after it reaches a critical size, and then each of the two unequal daughter apices will have differing rates of bifurcation as the tree (or branch) grows with time.

It could be argued that differences in bifurcation rates (and even flow rate) between daughter branches are a result of and not the cause of branch differences. Differences in apical sinks, initial meristem size, relative growth rates, total leaf surface, etc. would affect the

flow rate of materials through the daughter branches. Regardless of whether differing flow rates are the cause or only an effect of differential branching, the significant fact is that this simple regulatory mechanism can account for some complex patterns found in real trees.

Direct measurements of flow rates in branch systems, especially through new or young branches, would supply the facts necessary to support or refute our hypothesis of different flow rates. Some supportive data is presented by Zimmermann (1978) who showed that differences in the flow rates of dilute KCl solution through the xylem exist within one tree. He interprets this as the result of hydraulic constrictions between the trunk and lateral branches. These physiological constrictions are related to anatomical differences and result in differing, and presumably regulating, flow rates within the entire system. We should distinguish between the intrinsic flow rate of branches just after bifurcation, as is assumed in our model, and the "adaptive" flow rate which is established later and which is dependent upon branch growth subsequent to bifurcation. This latter flow rate is related to the weight of leaves attached to the distal branches and has been described by the "pipe model theory" (Shinozaki et al., 1964). In this theory the cross-sectional area of a stem axis is proportional to the total leaf surface it bears. This is supported by data which can be extracted from our measurements, since leaf area is directly related to the number of distal branch units, each of which bears a similar leaf cluster.

*Bifurcation ratios*—The results strongly suggest that bifurcation ratios may have little significance in interpreting adaptive geometry of botanical trees, since they show wide fluctuations when quite simple parameters are altered. Consequently, there is a non-linear distribution of branch number vs. order. Steingraeber et al. (1979) have already shown that the bifurcation ratio of *Acer* is quite different in different individuals in contrasted habitats. Tomlinson (1978) has also indicated that juvenile and adult forms, or different-sized individuals, of the same species may have dissimilar bifurcation ratios.

## LITERATURE CITED

- BELL, A. D., AND P. B. TOMLINSON. 1980. Adaptive architecture in rhizomatous plants. *Bot. J. Linn. Soc.* 80: 125–160.
- FISHER, J. B. 1978. A quantitative study of *Terminalia*-branching. In P. B. Tomlinson, and M. H. Zimmermann [eds.], *Tropical trees as living systems*, p. 285–320. Cambridge University Press, Cambridge.
- , AND H. HONDA. 1977. Computer simulation of branching pattern and geometry in *Terminalia* (Combrretaceae), a tropical tree. *Bot. Gaz.* 138: 377–384.
- , AND ———. 1979. Branch geometry and effective leaf area: a study of *Terminalia*-branching pattern. 1. Theoretical trees. *Amer. J. Bot.* 66: 633–644.
- HALLÉ, F., R. A. A. OLDEMAN, AND P. B. TOMLINSON. 1978. *Tropical trees and forests*. Springer-Verlag, Berlin.
- HONDA, H. 1971. Description of the form of trees by the parameters of the tree-like body; effects of the branching angle and the branch length on the shape of the tree-like body. *J. Theor. Biol.* 31: 331–338.
- , AND J. B. FISHER. 1978. Tree branch angle: maximizing effective leaf area. *Science* 199: 888–890.
- HORSFIELD, K. 1967. Morphology of the human bronchial tree. M.D. thesis, University of Birmingham, England.
- OHATA, S., AND T. SHIDEI. 1971. Studies of the branching structure of trees. I. Bifurcation ratio of trees in Horton's law. *Jap. J. Ecol.* 21:7–14.
- PHILLIPS, I. D. J. 1975. Apical dominance. *Ann. Rev. Plant Physiol.* 26: 341–367.
- SHINOZAKI, K., K. YODA, K. HOZUMI, AND T. KIRA. 1964. A quantitative analysis of plant form—the pipe model theory. I. Basic analyses. II. Further evidence of the theory and its application in forest ecology. *Jap. J. Ecol.* (Nippon Seitai Gakkaishi) 14: 97–105, 133–139.
- STEINGRAEBER, D. A., L. J. KASCHT, AND D. H. FRANK. 1979. Variation of shoot morphology and bifurcation ratio in sugar maple (*Acer saccharum*) saplings. *Amer. J. Bot.* 66: 441–445.
- STRAHLER, A. N. 1964. Quantitative analysis of watershed geomorphology. *Trans. Amer. Geophys. Un.* 38: 913–920.
- THORNLEY, J. H. M. 1977. A model of apical bifurcation applicable to trees and other organisms. *J. Theor. Biol.* 64: 165–176.
- TOMLINSON, P. B. 1978. Some qualitative and quantitative aspects of New Zealand divaricating shrubs. *N. Z. Jour. Bot.* 16: 299–309.
- WHITE, J. 1979. The plant as a metapopulation. *Ann. Rev. Syst. Ecol.* 10: 109–145.
- WHITNEY, G. G. 1976. The bifurcation ratio as an indicator of adaptive strategy in woody plant species. *Bull. Torrey Bot. Club* 103: 67–72.
- ZIMMERMANN, M. H. 1978. Hydraulic architecture of some diffuse-porous trees. *Can. J. Bot.* 56: 2286–2295.